

1 **Ecosystem model-based approach for modelling the**
2 **dynamics of ¹³⁷Cs transfer to marine plankton populations:**
3 **Application to the western North Pacific Ocean after the**
4 **Fukushima nuclear power plant accident**

5
6 **M. Belharet^{1,2}, C. Estournel² and S. Charmasson¹**

7 [1] (Institut de Radioprotection et de Sûreté nucléaire, ENV-PRP/SESURE/LERCM, 83507,
8 CS20330, La Seyne-Sur-Mer, France)

9 [2] (Laboratoire d'aérodologie (LA), UMR5560, CNRS – Université de Toulouse, UPS, 14
10 avenue Edouard Belin, 31400 Toulouse, France)

11 Correspondence to: M. Belharet (mokrane.belharet@gmail.com)

12
13 **Abstract**

14 Huge amounts of radionuclides, especially ¹³⁷Cs, were released into the western North Pacific
15 Ocean after the Fukushima nuclear power plant (FNPP) accident that occurred on 11 March
16 2011, resulting in contamination of the marine biota. In this study we developed a
17 radioecological model to estimate ¹³⁷Cs concentrations in phytoplankton and zooplankton
18 populations representing the lower levels of the pelagic trophic chain. We coupled this model
19 to a lower trophic level ecosystem model and an ocean circulation model to take into account
20 the site-specific environmental conditions in the area. The different radioecological
21 parameters of the model were estimated by calibration, and a sensitivity analysis to parameter
22 uncertainties was carried out, showing a high sensitivity of the model results, especially to the
23 ¹³⁷Cs concentration in seawater, to the rates of accumulation from water and to the
24 radionuclide assimilation efficiency for zooplankton. The results of the ¹³⁷Cs concentrations
25 in planktonic populations simulated in this study were then validated through comparison
26 with the some data available in the region after the accident. The model results have shown
27 that the maximum concentrations in plankton after the accident were about two to four orders
28 of magnitude higher than those observed before the accident depending on the distance from
29 FNPP. Finally, the maximum ¹³⁷Cs absorbed dose rate for phyto- and zooplankton
30 populations was estimated to be about $5 \times 10^{-2} \mu\text{Gy h}^{-1}$, and was, therefore, lower than the
31 predicted no effect dose rate (PNEDR) value of $10 \mu\text{Gy h}^{-1}$ defined in the ERICA assessment
32 approach.

1 **1 Introduction**

2 Huge amounts of radionuclides, especially ^{137}Cs , were released into the western North Pacific
3 Ocean after the Fukushima nuclear power plant (FNPP) accident that occurred on 11 March
4 2011 (UNCEAR, 2014).

5 Plankton populations, which play a prominent role in the input of many pollutants into the
6 aquatic food chain and are potentially important in the biogeochemical cycling of various
7 radionuclides in the ocean (Fowler and Fisher, 2004), were contaminated by these releases.

8 Data on ^{137}Cs in phytoplankton are rare especially due to difficulties in sampling. However,
9 recently Baumann et al (2015) reported ^{137}Cs data on suspended matter rich in marine
10 phytoplankton sampled in June 2011 off the Japanese coast (Buesseler et al., 2012) and
11 suggested that phytoplankton could have been a substantial source of ^{137}Cs for zooplankton
12 after the Fukushima accident.

13 Within a few months following the accident, zooplankton collected at some locations of the
14 western North Pacific showed enhanced levels of ^{137}Cs , even for the samples collected at the
15 farthest locations from FNPP, such as the S1 (47°N 160°E, 1,900 km from FNPP) and K1
16 (30°N 145°E, 900 km from FNPP) stations where the ^{137}Cs in zooplankton observed one
17 month after the accident were two orders of magnitude higher than before 11 March. Three
18 months after the accident, Buesseler et al. (2012) reported that the ^{137}Cs concentrations in
19 zooplankton located at 300-600 km from FNPP were two to three orders of magnitude higher
20 than before the accident. Even 10 months after the accident, the ^{137}Cs concentrations observed
21 in zooplankton, at 600-2,100 km away from FNPP, were still about one to two orders of
22 magnitude higher than in the pre-accident period (Kitamura et al., 2013).

23 Although these field data provide a general overview of the plankton contamination levels
24 after the FNPP accident, the lack of information on the contamination's temporal and spatial
25 evolution and the need for understanding the fate of radionuclides in the marine ecosystem,
26 necessary for the assessment of environmental and human health consequences, require the
27 adaptation of a modelling method.

28 The simple linear method based on the bioconcentration factor, defined as the ratio of the
29 amount of radionuclide in the organism divided by the concentration in the water, is the most
30 commonly used to assess the radionuclide concentration in marine biota (IAEA, 2004).
31 Despite its simplicity, this method is not appropriate in an accident situation since the main
32 underlying hypothesis, i.e. an equilibrium state between the radionuclide concentration in
33 water and biota, is not reached.

1 Rates of both radionuclide uptake and loss are known to be affected by species metabolism,
2 and it has been reported that a large part of the accumulated radionuclides by heterotrophic
3 marine biota comes from food (Thomann, 1981; Kasamatsu and Ishikawa, 1997; Zhao et al.,
4 2001 ; Rowan, 2013). Therefore, the characterization of the radionuclide distribution in these
5 components should be accompanied by ecological information such as species composition in
6 the ecosystem, population densities, rates of primary and secondary production, food
7 ingestion rate, etc. Such parameters are generally influenced by various environmental factors
8 (light, temperature, salinity, food availability, marine hydrodynamics) that vary quickly from
9 one site to another according to geographic location and morphological characteristics
10 (bathymetry, distance from the shore). Moreover, movements of radionuclides associated
11 with planktonic material are subject to physical transport processes, and are affected by
12 bioaccumulation, retention and subsequent food chain transfer, vertical migration of many
13 species, and passive sinking of biodebris. It follows that the relative importance of these
14 biological transport mechanisms will be a function of the oceanic biomass at any given
15 location (Fowler and Fisher, 2004).

16 Consequently, the effective consideration of all these factors implies that the modelling
17 approach of radionuclide transfer to marine biota should be driven by an ecosystem model
18 describing different ecological and physical processes and transfers between organisms in the
19 food web (Erichsen et al., 2013; Koulikov and Meili, 2003; Kryshev and Ryabov, 2000;
20 Kumblad et al., 2006; Sandberg et al., 2007).

21 In this study, we developed a generic radioecological model to estimate the ^{137}Cs
22 concentration in marine plankton populations. This model was applied to study ^{137}Cs transfer
23 to plankton populations in the western North Pacific after the FNPP accident and to compare
24 it with the pre-accident steady state situation. The NEMURO ecosystem model (Kishi et al.,
25 2007) was used to simulate the planktonic population dynamics in the area and to estimate
26 different ecological fluxes. It was coupled to the hydrodynamic SYMPHONIE model
27 (Marsaleix et al., 2008) in order to account for the impact of hydrodynamic and hydrologic
28 conditions on the dynamics of organic and inorganic materials. The ^{137}Cs concentrations in
29 seawater after the accident were obtained from dispersion numerical simulations.

30

31 **2 Material and methods**

32 The modelling method used in this study aims to estimate the activity concentration of ^{137}Cs
33 in different plankton populations, to analyse its sensitivity to the model parameter
34 uncertainties, and to understand the transfer mechanism and its relation with the ecological

1 functioning of the living organisms. It is based on three different models: (1) a 3D
2 hydrodynamic model simulating the movement of dissolved and particulate state variables of
3 the ecosystem model and estimating the physicochemical characteristics of seawater
4 (temperature, salinity), (2) an ecosystem model simulating the plankton biomasses and their
5 different metabolic rates and fluxes (e.g. primary production, excretion, grazing, mortality,
6 etc.), and (3) a mechanistic radioecological model simulating the ^{137}Cs concentration in
7 different plankton populations.

8

9 **2.1 Hydrodynamic modelling**

10

11 We used the three-dimensional SYMPHONIE ocean circulation model (Marsaleix et al.,
12 2009a, 2009b, 2012). This model has been widely used in the Mediterranean Sea to study
13 different marine processes related to coastal circulation (Estournel et al., 2003; Petrenko et al.,
14 2008), sediment transport (Ulses et al., 2008), larval dispersal (Guizien et al., 2012) and
15 plankton population dynamics (Auger et al., 2011; Herrmann et al., 2014). This model has
16 also been used, for the first time, in the western North Pacific Ocean to study the ^{137}Cs
17 dispersion after the FNPP accident (Estournel et al., 2012).

18 The numerical configuration used in this study was the same as the one reported in detail by
19 (Estournel et al., 2012), with 30 vertical irregular levels based on the sigma coordinate system
20 and characterized by an increase of resolution near the surface. The horizontal grid (Fig. 1)
21 corresponds to an orthogonal curvilinear system, with variable resolution increasing linearly
22 with the distance from FNPP (0.6 x 0.6 km near FNPP and 5 x 5 km at the open lateral
23 boundaries off Japan).

24

25 **2.2 Ecosystem modelling**

26 To properly represent the dynamics of the plankton populations exposed to the radioactive
27 contamination in our study area, the NEMURO (North-Pacific Ecosystem Model for
28 Understanding Regional Oceanography) biogeochemical model (Kishi et al., 2007) was
29 applied. This model, which has been extensively used in the western North Pacific region
30 (Aita et al., 2003; Hashioka and Yamanaka, 2007; Komatsu et al., 2007), consists of 11 state
31 variables with two size-classes of phytoplankton: small phytoplankton (PS) representing
32 small species such as coccolithophorids and flagellates, and large phytoplankton (PL)
33 representing diatoms. It includes three size-classes of zooplankton: small zooplankton (ZS)
34 such as ciliates and foraminifera, large zooplankton (ZL) (copepods), and predatory

1 zooplankton (ZP) such as krill and/or jellyfish. The other model state variables are: nitrate
 2 (NO_3), ammonium (NH_4), silicate ($\text{Si}(\text{OH})_4$), particulate organic nitrogen (PON), biogenic
 3 silica (Opal) and dissolved organic nitrogen (DON). The model structure and the different
 4 parameter values are presented in detail in (Kishi et al., 2007).

5

6 **2.3 Radioecological modelling**

7

8 **2.3.1 Phytoplankton**

9 The knowledge of the ^{137}Cs accumulation mechanisms in aquatic primary producers, mainly
 10 phytoplankton, is still vague. However, previous studies underlined that it is mostly
 11 transported into the cell by active absorption since it is an alkali metal analogue of potassium
 12 (Fukuda et al., 2014). Therefore, the dynamics of radionuclide concentration in phytoplankton
 13 populations is determined by a balance between radionuclide concentration in seawater, the
 14 biological half-life of clearance, and different processes affecting the population biomasses:

15

$$16 \frac{d[\text{Cs}]_p}{dt} = \mu_p [\text{Cs}]_w - (m_p + m_p^G) [\text{Cs}]_p - \frac{1}{B_p} \frac{dB_p}{dt} [\text{Cs}]_p - (\lambda_{p_B} + \lambda_{p_P}) [\text{Cs}]_p \quad (1)$$

17

18 Where $[\text{Cs}]_p$ is the ^{137}Cs concentration in the phytoplankton population (Bq g^{-1} wet weight),
 19 $[\text{Cs}]_w$ is the ^{137}Cs concentration in the seawater (Bq L^{-1}), B_p is the phytoplankton biomass
 20 ($\mu\text{molN L}^{-1}$), m_p and m_p^G are, respectively, the natural mortality rate and the rate of mortality
 21 due to the grazing (d^{-1}), λ_{p_B} and λ_{p_P} are, respectively, the biological depuration rate of ^{137}Cs
 22 from phytoplankton and the ^{137}Cs physical decay rate (d^{-1}), and μ_p is the ^{137}Cs accumulation
 23 rate by the phytoplankton ($\text{L g}^{-1} \text{d}^{-1}$).

24 In the NEMURO ecosystem model, the phytoplankton population growth rate is given by the
 25 equation:

$$26 \frac{1}{B_p} \frac{dB_p}{dt} = P - exc_p - R_p - m_p - m_p^G \quad (2)$$

27

28 Where exc_p and R_p are, respectively, the phytoplankton excretion and respiration rates (d^{-1}),
 29 and P the gross primary production rate (d^{-1}). After rearrangement we obtain from Eq. (1) and
 30 Eq. (2) :

$$31 \frac{d[\text{Cs}]_p}{dt} = \mu_p [\text{Cs}]_w - (P - exc - R + \lambda_p) [\text{Cs}]_p \quad (3)$$

32

1 2.3.2 Zooplankton

2 The dynamics of radionuclide concentration in consumers reflects the variation over time of
3 the radionuclide intake from both water and food. Therefore, the differential equation
4 describing the dynamics of ^{137}Cs concentration in the zooplankton populations can be written
5 as:

$$7 \frac{d[\text{Cs}]_z}{dt} = \mu_z [\text{Cs}]_w + AE_z \sum_{j=1}^N IR_{j \rightarrow z} [\text{Cs}]_j - \left(m_z + m_z^G + \lambda_{zB} + \lambda_{zP} + \frac{1}{B_z} \frac{dB_z}{dt} \right) [\text{Cs}]_z \quad (4)$$

8
9 Where $[\text{Cs}]_z$, $[\text{Cs}]_j$ and $[\text{Cs}]_w$ represent, respectively, the ^{137}Cs concentrations in
10 zooplankton, in prey index j ($\text{Bq g}^{-1} \text{ ww}$) and in seawater (Bq L^{-1}), B_z is the zooplankton
11 biomass ($\mu\text{molN L}^{-1}$), μ_z is the ^{137}Cs accumulation rate by zooplankton population (d^{-1}), AE_z
12 is the assimilation efficiency of ^{137}Cs by zooplankton, $IR_{j \rightarrow z}$ is the ingestion rate of prey index
13 j by the zooplankton, N represents the number of prey populations present in the area that are
14 available for the zooplankton, λ_{zB} and λ_{zP} are, respectively, the biological depuration rate
15 (d^{-1}) of the ^{137}Cs by the zooplankton and the ^{137}Cs radioactive physical decay rate (d^{-1}), and
16 m_z and m_z^G are, respectively, the zooplankton natural and grazing mortality rates (d^{-1}).

17 The zooplankton population growth rate is modelled in the NEMURO model as follows:

$$19 \frac{1}{B_z} \frac{dB_z}{dt} = \left(\sum_{j=1}^N IR_{j \rightarrow z} \right) - exc_z - ege_z - m_z - m_z^G \quad (5)$$

20
21 Where exc_z and ege_z are, respectively, the excretion and egestion rates (d^{-1}). After
22 rearrangement of equations modelled in the NEMURO model we obtain:

$$24 exc_z + ege_z = (1 - b) \sum_{j=1}^N IR_{j \rightarrow z} \quad (6)$$

25
26 Where b is the growth efficiency of zooplankton ($Beta_z$ in Kishi et al. (2007)). By inserting
27 Eq. (5) into Eq. (4), and considering Eq. (6), we can write:

$$29 \frac{d[\text{Cs}]_z}{dt} = \mu_z [\text{Cs}]_w + AE_z \left(\sum_{j=1}^N IR_{j \rightarrow z} [\text{Cs}]_j \right) - \left(\lambda_z + b \sum_{j=1}^N IR_{j \rightarrow z} \right) [\text{Cs}]_z \quad (7)$$

31 2.4 Model simulation

1 The ocean circulation model (OCM) was run from February 2010 to January 2013. The
2 currents, vertical diffusivities and temperature fields were then used to force the ecosystem
3 model and spun-up for 3 years by repeating the same forcing data for the first two years. For
4 this study, we used the results of the two last simulated years (February 2011 to December
5 2012), when a quasi-steady state was reached.

6 To assess the effect of the accident on the planktonic populations, two different simulations
7 were carried out: 1) the real (accidental) situation with presence of contaminated waters due
8 to the accident occurred on 11 March 2011, and 2) a non-accidental situation by assuming
9 homogeneous ^{137}Cs concentration in seawater over the whole simulation period.

10 Before the accident date (11 March 2011), the seawater ^{137}Cs concentration for the western
11 North Pacific Ocean ranged from 1 to 2 mBq L^{-1} (Povinec et al., 2013) . For the purposes of
12 the modelling, a constant ^{137}Cs concentration in seawater of 2 mBq L^{-1} is assumed throughout
13 the study area. In the accidental situation, we used, as of 11 March 2011, the ^{137}Cs
14 concentrations in seawater obtained from the dispersion simulation carried out by Estournel et
15 al. (2012), in which the amount of atmospheric deposition included was 0.26 PBq within a
16 radius of 80 km. The direct leakage was about 5.5 PBq released between 12 March and 30
17 June 2011. The simulation was extended until 31 December 2012, the inverse method
18 described in Estournel et al., (2012) and used to calculate the source term in the first three
19 months after the accident was applied to the whole period. After June 2011, the
20 concentrations at the two outlets of the nuclear power plant were simplified to a linear
21 decrease from 40 and 20 Bq L^{-1} on 1st July 2011 to 8 Bq L^{-1} for both outlets at the end of 2011
22 and then remained constant at this value for 2012. However, no other additional source (e.g.
23 terrestrial runoff, rivers flow, etc) has been considered in this simulation.

24

25 **2.5 Model calibration and sensitivity analysis**

26 The radioecological parameters related to plankton are very scarce, and are often associated
27 with considerable uncertainties. In this study, a temporal series of the ^{137}Cs concentration in
28 zooplankton collected at Sendai Bay between June 2011 and December 2013 and reported in
29 Kaeriyama et al. (2014) was used to calibrate the model and estimate the different
30 radioecological parameters. However, because of non-indication of the zooplankton taxa
31 composition, we used for the purpose of modelling a weighted average of ^{137}Cs
32 concentrations in the three-zooplankton groups.

33 To assess the sensitivity of the calibrated parameters, we investigated a sensitivity analysis of
34 the radioecological model using the classical one-parameter-at-a-time analysis (OAT). The

1 choice of this quantitative method can be justified by its simplicity and by the absence of any
 2 interactive effects among parameters. In this local approach, the single parameter variation
 3 effect is estimated by increasing and decreasing each parameter in equations (3) and (7) by
 4 10%, while keeping all the others fixed at their nominal values. The sensitivity S_p associated
 5 with each parameter p was computed as the percentage of change in activity generated by the
 6 parameter variation:

$$8 \quad S_p(\%) = \frac{E(p) - E}{E} * 100 \quad (8)$$

9
 10 Where $E(p)$ is the prognostic variable value (here, the ^{137}Cs concentration in plankton
 11 populations) when the parameter p is set to its changed value (10% higher or lower than its
 12 calibrated value), and E is the value of the prognostic variable in the baseline run (i.e., all
 13 parameters at their calibrated values).

14

15 **2.6 Absorbed dose rate**

16 To assess the biological effects of the ^{137}Cs ionizing radiation on the plankton populations, we
 17 calculated the absorbed dose rate from internal and external pathways using the ERICA
 18 graded approach (Brown et al., 2008). This approach consists in converting the ^{137}Cs
 19 concentration in plankton populations and in seawater to the internal and external absorbed
 20 dose rates, respectively, using the so-called “Dose Conversion Coefficients”, which are
 21 specific for each radionuclide-organism combination. The different dose rates are calculated
 22 as follows, assuming that the organisms are freely floating in the water column without any
 23 contact with sediment:

24

$$D = D_{int} + D_{ext}$$

$$D_{int} = DCC_{Cs-pk} [Cs]_{pk}$$

$$D_{ext} = DCC_{Cs-w-pk} [Cs]_w$$

25

26 Where D , D_{int} , D_{ext} are, respectively, the total, the internal and the external dose rates (μGy
 27 h^{-1}), $[Cs]_{pk}$ and $[Cs]_w$ are, respectively, the ^{137}Cs concentration in plankton population and
 28 seawater (in Bq kg^{-1}), DCC_{Cs-pk} is the dose conversion coefficient for the internal exposure,

1 and $DCC_{CS-w-pk}$ represents the dose conversion coefficient for external exposure (in μGy
2 h^{-1} per Bq kg^{-1}).

3 The DCC parameter values for phytoplankton and zooplankton used in this study are obtained
4 from the coastal aquatic ecosystem DCCs reported in (Vives i Batlle et al., 2004). The values
5 of these parameters are summarized in Table 1.

6

7 **3 Results and discussions**

8

9 **3.1 Validation of the ecosystem model, and zooplankton taxonomic** 10 **compositions**

11 The seasonal variations in phytoplankton and zooplankton biomasses were presented for three
12 different areas classified according to latitude: the subtropical region (latitude $< 35^{\circ}\text{N}$), the
13 transition region ($35^{\circ}\text{N} < \text{Latitude} < 39^{\circ}\text{N}$), and the subarctic region (Latitude $> 39^{\circ}\text{N}$) (Fig.
14 1). The ecosystem model outputs are expressed in $\mu\text{mol N L}^{-1}$, their conversion to the
15 chlorophyll-a unit is carried out using a typical C:chl ratio of 50, and a C:N ratio of 133/17
16 (Kishi et al., 2007).

17 The monthly medians of the spatial chlorophyll-a concentration averaged over a 50 m deep
18 layer were used to compare model results for the period (2011-2012) with the twenty years of
19 climatology field data (1990-2010) (Fig. 2: A, C, E) derived from the Japan Oceanographic
20 Data Center (JODC) dataset (available at: <http://www.jodc.go.jp>). In all areas, the temporal
21 evolution of the chlorophyll standing stocks showed a seasonal cycle with higher median
22 values in spring (April-May) and autumn (October-November). This seasonal cycle is less
23 marked in the subtropical region than in the two other regions. The simulated chlorophyll-a
24 concentration medians varied from less than 0.5 mg.m^{-3} in all regions in winter to
25 approximately 1, 1.5 and 3 mg m^{-3} in spring in the subtropical, the transition and the subarctic
26 regions, respectively. These values of the chlorophyll-a concentrations are in general
27 consistent with the field data, and show the same seasonal variability [Wilcoxon ranksum test
28 ($\alpha = 0.05$): $P = 0.88$].

29 The total zooplankton biomass and its taxonomic composition are presented in Fig. 2 (B, D,
30 F) for the three regional areas described above. The simulated zooplankton biomasses showed
31 an annual seasonality in the three regions, with minimum values in winter and peaks in spring
32 and autumn. The zooplankton biomasses showed latitudinal variations with greater biomass in
33 the subarctic region (from 200 mg m^{-3} wet weight in winter to about 700 mg m^{-3} wet weight

1 in late spring), followed by the transition region (from $150 \text{ mg m}^{-3} \text{ ww}$ to about 500 mg m^{-3}
2 ww) and the subtropical region (from $100 \text{ mg m}^{-3} \text{ ww}$ to about $300 \text{ mg m}^{-3} \text{ ww}$).
3 In the subtropical region, the taxonomic composition of zooplankton biomass was dominated
4 by large zooplankton with about 40%, followed by small and predatory zooplankton each
5 accounting for 30% of the total biomass.
6 In the transition region, the seasonal cycle of zooplankton composition was more pronounced.
7 In winter, the zooplankton was represented by 40% of large zooplankton, and 30% of small
8 and predatory zooplanktons. In spring, the zooplankton biomass was dominated by large
9 zooplankton (60% ZL and 20% for both ZS and ZP). From late spring until early autumn, the
10 zooplankton composition changed progressively with a decrease of the ZL proportion, to be
11 composed of 40% ZP and 30% of ZS and ZL in early autumn.
12 In the subarctic region, the proportions of small zooplankton, large zooplankton and predatory
13 zooplankton were, respectively, 25%, 35% and 40% in winter, 10%, 70% and 20% in spring,
14 and 20%, 35% and 45% in late summer and early autumn.

15

16 **3.2 Model calibration**

17 The result of the calibration is shown in Fig. 3, and the final estimated radioecological
18 parameters are summarized in Table 2. The phytoplankton elimination rates estimated from
19 this calibration (0.5 d^{-1}) were very similar to that calculated using the allometric relationship
20 reported by Vives i Batlle et al. (2007) (0.58 d^{-1}). For the zooplankton, the obtained values
21 ranged from 0.03 to 0.11 d^{-1} , and are also in good agreement with the literature values [
22 Thomann (1981): 0.03 d^{-1} ; Vives i Batlle et al. (2007): 0.056 d^{-1}].

23 The ^{137}Cs assimilation efficiency by zooplankton calibrated in this study was 0.75. This value
24 is similar to that used by Brown et al. (2006), and is slightly higher than 0.63 observed by
25 Mathews and Fisher (2008) for the crustacean zooplankton *Artemia salina*.

26 The rates of ^{137}Cs direct accumulation from water by zooplankton found in this study were
27 about $5 \times 10^{-4} \text{ L g}^{-1}$ for small and large zooplankton, and about $0.001 \text{ L g}^{-1} \text{ d}^{-1}$ for predatory
28 zooplankton. The accumulation rate corresponding to phytoplankton was 0.015 for both
29 groups.

30 However, for the calibration we used zooplankton data from coastal areas presented in
31 (Kaeriyama et al., 2014). According to these authors, zooplankton gut content in these areas
32 may contain particles with high ^{137}Cs levels, which could affect the calibrated values.
33 Consequently, over-estimations in ^{137}Cs concentrations in these populations could be
34 generated especially in the open ocean where the particles contribution is generally negligible.

1
2
3
4
5
6
7
8
9
10
11
12
13
14
15
16
17
18
19
20
21
22
23
24
25
26
27
28
29
30
31
32
33
34

3.3 Sensitivity analysis

The sensitivity of the estimated ^{137}Cs activity concentrations in different plankton groups to uncertainty in the parameters of equations (3) and (7) calibrated to field data at Sendai Bay was tested using the OAT method, and the results are shown in Fig. 4.

For all plankton groups, the ^{137}Cs activity estimates showed a great sensitivity to the ^{137}Cs concentration in seawater, with an activity change of 10% for a 10% change in the seawater ^{137}Cs concentration. The ^{137}Cs activity in seawater used in this study was obtained from the numerical simulations of the ^{137}Cs dispersion using the SYMPHONIE circulation model. One can imagine that all potential biases associated with this simulation would generate the same ranges of error in the results concerning the ^{137}Cs concentration in plankton. It is, therefore, clearly important to take into consideration all these errors when interpreting the results of the radioecological model.

The ^{137}Cs activity estimates in the phytoplankton groups are very sensitive to the accumulation rate from water (10% change for a 10% change in the parameter), and are moderately sensitive to the elimination and primary production rates (5-7% change in the opposite sense), whereas the sensitivity to the daily respiration rate did not exceed 1%. The primary production rate is, therefore, the most important ecological parameter in the estimation of ^{137}Cs concentrations in phytoplankton. It allows dilution of the ^{137}Cs concentrations in phytoplankton by promoting the growth of its populations.

For all zooplankton groups, the activity estimates were most sensitive to the change in the ^{137}Cs assimilation efficiency (AE), with an activity change of about 9% for both small and large zooplankton. For predatory zooplankton, the activity change was slightly above 10%, which can be explained by the direct effect of the AE parameter on ZP and the indirect effect due to the change in ZS and ZL that are preyed on by ZP.

The sensitivity to the population growth efficiency (b) was also significant with about 7% of change. This ecological parameter, which affects the zooplankton population growth and consequently plays a role in the dilution of their ^{137}Cs concentrations, is associated with substantial uncertainty. Sushchenya (1970) reported values ranging from 4.8 to 48.9%. The value used in this study was 30% (Kishi et al., 2007). One can expect, therefore, an overestimation of up to 45% or an underestimation of up to 60% in the estimates of zooplankton ^{137}Cs concentrations.

1 The sensitivity to the direct accumulation rate of ^{137}Cs from water by zooplankton (μ_z) was
2 relatively low (< 4% for the three groups of zooplankton). This can be related to the lower
3 proportion of contamination coming from water compared to that coming from food. The
4 variation in the depuration rate induced a relatively moderate change of 5%.
5 The sensitivity of the ^{137}Cs activity estimates in the three groups of zooplankton to parameters
6 related to their different preys is also not negligible. The proportions of change varied from
7 1% to 9% depending on the zooplankton group and the parameter in question. For example,
8 the sensitivity of the ^{137}Cs concentration in ZS to the PS accumulation rate (μ_{ps}), the
9 elimination rate (λ_{ps}), and the primary production rate (P) were 9%, 5% and 7%, respectively.
10 This sensitivity analysis showed that the parameters related to the two groups of
11 phytoplankton are very important for the estimation of the ^{137}Cs concentration in all plankton
12 groups. Therefore, these parameters are key determinants of the radionuclide concentration in
13 all marine animals of the pelagic food chain (Mathews and Fisher, 2008). Consequently, the
14 experimental determination of these parameters, often neglected due to the difficulties
15 characterizing the measurement of radionuclides in phytoplankton, is of the greatest
16 importance.

17

18 **3.4 Radioecological model validation**

19

20 The simulation results corresponding to the spatial distribution of the weighted average of
21 ^{137}Cs concentrations in the three-zooplankton groups (ZS, ZL, ZP) are presented in Fig. 5.
22 These results are shown for 6 different dates from June 2011 to August 2012, and are
23 compared to the few field observations available in the area (Buesseler et al., 2012;
24 Kaeriyama et al., 2014; Kitamura et al., 2013). Some field data reported in the unit of Bq kg^{-1}
25 dry weight are converted to Bq kg^{-1} wet weight using dry to weight ratio of 0.2 (Buesseler et
26 al., 2012).

27 In general, these results illustrated the good agreement between measured and simulated
28 results, which is confirmed by the Wilcoxon rank-sum statistical test ($P > 0.05 \rightarrow$ non-
29 significant difference). Nevertheless, some points showed significant discrepancies between
30 measured and simulated concentrations, as in the case of (36°N , 144°W) on 3-18 June 2011
31 (Fig. 5 a) where the observed concentration was two orders of magnitude higher than the
32 simulated one. A large part of this difference could be due to a spatial shift of the
33 contaminated plume in the dispersion model. Indeed, the coastal waters off Japan are very
34 energetic, especially with the interaction between the cold Oyashio current moving southward

1 and the warm Northward Kuroshio current, generating very complex physical structures
2 (eddies, tidal forces, etc), which are generally less well represented by the hydrodynamics
3 models leading to some spatial shifts between the simulated ^{137}Cs concentrations in seawater
4 used in this simulation and the real field concentrations.

6 **3.5 Amplification of the ^{137}Cs concentration in plankton populations following** 7 **the FNPP accident**

8 To assess the contamination level of plankton populations in 2011, we calculated a ratio (R)
9 of the ^{137}Cs concentration in phytoplankton (the weighted average of PS and PL) and
10 zooplankton (the weighted average of ZS, ZL and ZP) in the accidental situation to its
11 concentration in these populations in the non-accidental situation. The results of the temporal
12 evolution of these ratios for different distances from FNPP are shown in Fig. 6.

13 The ratios for phytoplankton and zooplankton are very similar spatially and temporally. After
14 the accident, the ratio increased rapidly until reaching a maximum, whose the value and the
15 time required to reach it are variable following the distance from FNPP. The results showed
16 that the time, calculated from the accident date, required to reach the maximum value increase
17 with distance from FNPP, going from about 1 month for the populations located at less than
18 30 km from FNPP to about 6 months for those located at 500 m from FNPP. The maximum
19 value, in turn, decreased with the distance from FNPP (about 10^4 at 0-30 km from FNPP to
20 slightly lower than 10^2 at 400-500 km from FNPP).

21 After reaching the peak, the ratios progressively decreased over time but remained relatively
22 high at the end of 2011 especially in the sectors situated at less than 50 km from FNPP where
23 the ratio was still higher than 10.

24 The rapid decrease of ^{137}Cs in planktonic populations one year after the accident in the major
25 parts of the study area can be explained by the different processes related to both population
26 ecological functioning (cells growth and death, biological elimination) and the surrounding
27 environment conditions especially by the horizontal and vertical mixing due to the ocean
28 hydrodynamics. Indeed, FNPP is located in an area where the east-flowing Kuroshio current
29 and the southwest-flowing Oyashio current mix, generating complicated nearshore currents
30 and mesoscale eddies (Buesseler, 2014), thereby favouring dispersion, regeneration, and thus
31 dilution, of the contaminated planktonic populations in the area.

32 Referring to the biogeochemical cycle in the pelagic environment, part of the contaminated
33 populations would be transferred to the pelagic higher trophic levels (planktivorous fishes,
34 squids, etc.) by predation leading to transfer of this contamination along various trophic

1 chains. The other part will generate, after dying, large aggregated particles, known
2 collectively as marine snow, which can reach the deep waters (Asper et al., 1992) and thus
3 contribute to the contamination of sediment and benthic organisms, especially in the coastal
4 area. This phenomenon was observed in the Mediterranean Sea a few days after the
5 Chernobyl accident, generating a rapid transport of some radionuclides from surface waters to
6 a depth of 200 m (Fowler et al., 1987) . This process could be expected in the Japanese
7 coastal area characterized by very high levels of contamination especially around FNPP.

10 **3.6 Apparent concentration ratio (aCR)**

11 The concentration ratio ($L\ kg^{-1}$) is defined as the ratio of radionuclide in the organism (Bq
12 kg^{-1} wet weight) divided by its concentration in the water ($Bq\ L^{-1}$). The dynamics of the
13 calculated apparent concentration ratios (aCR) for small phytoplankton, small zooplankton
14 and predatory zooplankton populations throughout the study area and for populations located
15 within a radius of 30 km from FNPP over the year 2011 are shown in Fig. 7. These apparent
16 concentration ratios are estimated for the two different situations described above (see Section
17 2.4).

18 The spatial median of the apparent concentration ratios in the non-accidental situation (i.e. the
19 steady state situation) was between 20 and 30 $L\ kg^{-1}$ wet weight for small phytoplankton and
20 between 10 in winter to slightly more than 30 $L\ kg^{-1}$ during the rest of the year for small
21 zooplankton. In the case of predatory zooplankton, the concentration ratio was a little higher,
22 ranging from 10 to about 40 $L\ kg^{-1}$ wet weight. These values are in good agreement with the
23 reported data on plankton concentration ratios in marine ecosystems, which generally range
24 from 6 to 40 $L\ kg^{-1}$ wet weight in steady state conditions (Fowler, 1977; IAEA, 2004;
25 Kaeriyama et al., 2008). In the sector situated at less than 30 km from FNPP (Fig. 7), the
26 concentration ratio was almost constant and seasonal variability was very less pronounced,
27 with about 25 $L\ kg^{-1}$ for PS and 30-40 for ZS and ZP. This constancy in the estimated
28 concentration ratios for the populations located at less than 30 km compared to those
29 estimated for the whole study area, where a substantial decrease in the concentration ratio was
30 observed during winter, can be related to the clear differences in food ingestion rates observed
31 in this period between the two locations (Fig. 8). In winter, the zooplankton ingestion rates
32 estimated for the populations located at less than 30 km were higher than those estimated for
33 the whole study area, due essentially to the spatial heterogeneity characterizing the whole
34 study area in terms of food availability, with presence of some **less productive** regions such

1 as the subtropical zone where the planktonic biomasses were generally very low (see Section
2 3.1).

3 At the time of the releases and immediately after the accident, the concentration ratio
4 decreased rapidly for all plankton groups. This is mainly due to the sudden arrival of highly
5 contaminated waters in these areas where the living plankton populations were not yet
6 contaminated. This phase was less marked for small phytoplankton compared to the groups of
7 zooplankton, due to the fact that phytoplankton accumulates ^{137}Cs only from water whereas in
8 the case of zooplankton an important part of the contamination arises from food, a process
9 requiring some time. For the populations located at less than 30 km from FNPP the dramatic
10 decrease in the concentration ratio in March was even more intense and longer. The estimated
11 time needed for these populations to regain the equilibrium was about 5-10 days for PS, 30
12 days for ZS and about 50 days for ZP. The decreasing phase in concentration ratio was
13 directly followed by an increasing phase reflecting the progressive accumulation of ^{137}Cs by
14 plankton organisms.

15

16 **3.7 Relative accumulation of ^{137}Cs from diet by zooplankton**

17 The dynamics of ^{137}Cs fraction accumulated from diet by zooplankton populations is
18 estimated for both accidental and non-accidental situations and in the two spatial scales (Fig.
19 9). This fraction remained stable in the case of zooplankton living at less than 30 km from
20 FNPP and represented more than 80% in the case of ZS, 90% in the case of ZL, and 98% in
21 the case of ZP. These results indicated that the major part of accumulated ^{137}Cs by these
22 populations is coming from food, which is consistent with the research conducted by
23 Baumann et al. (2015), who postulated that the dietary route could be largely responsible for
24 the ^{137}Cs bioaccumulated by the zooplankton collected off Japan three months after the
25 accident.

26 The accident effect was only briefly apparent with a slight decrease of this proportion.

27 Conversely, the proportion estimated for zooplankton populations living in the whole area
28 revealed a decline in winter, especially in the case of ZS for which this proportion decreased
29 to 30%. Because of the non-decrease in the ^{137}Cs concentration in PS during this period (Fig.
30 10), the decrease in the relative accumulation by ZS from diet could be related to the decrease
31 in the food ingestion rate (Fig. 8). No apparent effect of the accident on the ^{137}Cs fraction
32 accumulated from diet was observed at this large spatial scale.

33

34 **3.8 Trophic transfer factor**

1 The trophic transfer factor (TTF), defined as the ratio of radionuclide concentration in the
2 predator to its concentration in prey, was calculated for each zooplankton group. The small
3 zooplankton (ZS) has only one prey (small phytoplankton), therefore the TTF was calculated
4 directly by dividing the ^{137}Cs concentration in the ZS by its concentration in the PS. In the
5 case of large and predatory zooplanktons that have more than one prey (3 for each one), we
6 considered the weighted average of the ^{137}Cs concentration in preys related to each
7 zooplankton group.

8 Boxplots of predicted TTFs over 2011 for the three zooplankton groups in the accident and
9 steady state situations are shown in Fig. 11 for the two spatial scales described above.

10 The predicted TTF medians in the steady state situation for ZS, ZL and ZP were, respectively,
11 about 1.5, 1.7 and 1.2 in the sector 0-30 km from FNPP, and about 1.2, 1.45 and 1.1 in the
12 whole study area. The TTF values calculated for the whole study area were slightly lower
13 than those of the 0-30 km sector, reflecting the variability in ingestion rate and diet
14 composition between the two spatial scales (Fig. 8). The lower values of ZP TTFs compared
15 to the two other zooplankton groups may also be due to differences in their respective
16 ingestion rate values. The correlation coefficient r between the modelled TTF related to each
17 zooplankton group in the steady state conditions and their corresponding ingestion rates
18 showed a good correlation for the three groups of zooplankton and in both considered spatial
19 scales (Table 3).

20 The predicted TTFs in the accident situation were similar to those predicted in the steady state
21 situation when considering the whole study area. This is due to the fact that, in the farthest
22 sites from FNPP, where the contamination was not very high, the return to equilibrium
23 occurred more rapidly, leading to TTFs similar to those observed before the accident although
24 the concentrations in the predator and its preys were higher than during the pre-accident
25 period. In the sector 0-30 km from FNPP, the predicted TTFs in the accidental situation were
26 lower than those predicted in the steady state situation (non-accidental situation). This is due
27 to the persistence of the non-equilibrium state and the high ^{137}Cs concentrations in seawater in
28 this area, and to the fact that zooplankton accumulates ^{137}Cs mainly from food leading to a
29 delay in its contamination compared to its preys.

30 In turn, the correlation coefficients between predicted TTFs and ingestion rates in the accident
31 situation showed a very slight decrease when considering the whole study area, and a
32 considerable decrease when considering only the sector 0-30 km from FNPP. This means that
33 the instability and the non-steady state conditions characterizing the post-accident period had
34 significant effects on this correlation.

1 Previous works suggested that radiocesium is the only trace element apart from Hg that may
2 be potentially biomagnified along food chains (Harmelin-Vivien et al., 2012; Heldal et al.,
3 2003; Zhao et al., 2001). In our study, the modelled TTFs were generally higher than the
4 unity for all zooplankton groups, showing evidence of biomagnification potential at this
5 trophic level. Mathews and Fisher (2008) reached the same general conclusion for the
6 crustacean zooplankton *Artemia salina* feeding on phytoplankton, and reported that TTFs are
7 directly related to the food ingestion rates, and that a consistent capacity for biomagnification
8 exists when the food ingestion rate is high.

9

10 **3.9 Absorbed dose**

11 The estimation of the absorbed dose rate ($\mu\text{G h}^{-1}$) is an essential step enabling media/biota
12 activity concentrations to be interpreted in terms of potential effect (Beresford et al., 2007) .

13 The calculated dose rates received by phytoplankton and zooplankton populations located at
14 less than 30 km from FNPP over 2011 are shown in Fig. 12. The external dose rate was about
15 7 times higher than the internal dose rate for phytoplankton, and about 5 times higher than the
16 internal dose rate in the case of zooplankton, resulting in similarity between the total and the
17 external dose rates. The total dose rates for phyto- and zooplankton were also very similar,
18 whereas the internal dose was higher for zooplankton than for phytoplankton.

19 For both phyto- and zooplankton, in the steady state conditions before the accident, the dose
20 rates were about $10^{-6} \mu\text{Gy h}^{-1}$. The maximum value was reached one month after the accident
21 with about $0.05 \mu\text{Gy h}^{-1}$. From this date, the dose rates decreased progressively to reach about
22 $5 \times 10^{-5} \mu\text{Gy h}^{-1}$ at the end of 2011. The calculated internal dose rates for zooplankton in June
23 2011 were about $10^{-4} \mu\text{Gy h}^{-1}$, and were, therefore, about 5 times greater than those reported
24 by Fisher et al.(2013) for copepods and euphausiids collected 30-600 km off Japan. This
25 difference is mainly due to the fact that in this study the dose rates were calculated for the
26 populations located at 0-30 km from FNPP, where the activity level of ^{137}Cs was higher.

27 The maximum dose rates calculated here were very low relative to the benchmark value
28 corresponding to $10 \mu\text{Gy h}^{-1}$ as suggested by the ERICA approach (Beresford et al., 2007),
29 signifying that the ^{137}Cs levels were too low to cause a measurable effect on these plankton
30 populations. However, this conclusion concerns only ^{137}Cs , we ignore whether the ionizing
31 radiation doses due to the other radionuclides released in high quantities following the FNPP
32 accident, such as short-lived nuclides ^{132}Te , ^{131}I and ^{90}Sr , can generate any effect on these
33 populations. Finally, it is important to note that this finding may be more representative of the
34 average conditions characterizing the area located up to 30 km from FNPP, however in close

1 vicinity to the FNPP (e.g. FNPP Port), the planktonic populations could have been exposed to
2 more intense and more persistent doses that could generate higher deleterious effects on these
3 populations.

4 **4 Conclusions**

6 We presented a modelling approach based on an ecosystem model to estimate the ^{137}Cs
7 activity in marine plankton populations following the Fukushima nuclear power plant (FNPP)
8 accident, and to understand the effect of this accident on the different processes related to the
9 radiocesium transfer in the planktonic trophic levels. This kind of model enables calculation
10 of the non-equilibrium dynamic processes of radionuclide transfer for the biological
11 compartments taking into account the dynamics of the biomass and the spatio-temporal
12 variability in the ecological parameters and environmental conditions (Sazykina, 2000).

13 The radioecological parameters were estimated by calibration, and the model was validated
14 with observed ^{137}Cs data in zooplankton two months and ten months after the accident. This
15 study showed that the maximum values of the ^{137}Cs concentrations in phytoplankton and
16 zooplankton populations were mainly reached one month after the accident and were about
17 two to four orders of magnitude higher than those observed before the accident depending on
18 the distance from FNPP. On the other hand, It should be important to note that although the
19 model results indicate that the spatio-temporal dynamics of ^{137}Cs concentrations in
20 zooplankton populations in non-accidental conditions are mainly depending on the food
21 availability (i.e. phytoplankton biomasses in the area), with an apparent decrease of cesium
22 concentrations in these populations during the limited-food conditions (e.g. winter), this
23 finding has to be verified and validated by multi-years field observations once these data are
24 available.

25 Contrary to Baumann et al. (2015) who did not observe any biomagnification between
26 phytoplankton and zooplankton collected three months after the accident, our study
27 highlighted a modest biomagnification potential between the zooplankton groups, since the
28 calculated trophic transfer factors were slightly higher than unity. The result obtained by
29 Baumann et al. (2015) could be due to the fact that, three months after the accident, the
30 equilibrium has not been reached (Kaeriyama et al., 2014) resulting in some delay in predator
31 (zooplankton) contamination compared to its preys (phytoplankton) since the major part of
32 the bioaccumulated ^{137}Cs by zooplankton is coming from food. Further analysis covering a
33 longer time series of contamination levels in zooplankton and phytoplankton are therefore
34 required to better understand the biomagnification potential of these species. In our study, the

1 TTF has been calculated over the full year 2011, but one has to be careful in interpretation of
2 this result since it is not yet validated using the field data.

3 Although the contamination degrees characterizing the seawater and the plankton populations
4 following the FNPP accident were high, the maximum ^{137}Cs dose rates calculated for both
5 phyto- and zooplankton were about $5 \times 10^{-2} \mu\text{Gy h}^{-1}$, they remained lower than the benchmark
6 value considered in this study, which corresponds to the incremental screening dose rate of 10
7 $\mu\text{Gy h}^{-1}$ defined in the ERICA assessment approach (Beresford et al., 2007). However, it is
8 important to note that the dose rate calculated in this study concerns only ^{137}Cs , and that we
9 ignore, at this stage, whether the ionizing radiation doses due to the other radionuclides
10 released in high quantities following the FNPP accident can generate any effect on these
11 populations, even though all previous studies have shown that the radioactivity levels in
12 marine biota have generally been below the levels necessary to cause a measurable effect on
13 populations (e.g. Vives i Batlle, 2015).

14
15

16 **Acknowledgements:**

17 We warmly thank Caroline Ulses, Thomas Duhaut, Cyril Nguyen and Patrick Marsaleix of
18 the Laboratoire d'Aérodologie (CNRS and Toulouse university) for their continuous assistance.
19 This work was carried out in the frame of the AMORAD project (French state financial
20 support managed by the National Agency for Research allocated in the "Investments for the
21 Future" framework programme under reference ANR-11-RSNR-0002). This work is also part
22 of the EC 7th Framework project COMET (Coordination and iMplementation of a pan-Europe
23 instrument for radioecology).

24

1 **References**

- 2 Aita, M. N., Yamanaka, Y. and Kishi, M. J.: Effects of ontogenetic vertical migration of
3 zooplankton on annual primary production - using NEMURO embedded in a general
4 circulation model, *Fish. Oceanogr.*, 12(4-5), 284–290, doi:10.1046/j.1365-
5 2419.2003.00261.x, 2003.
- 6
- 7 Asper, V. L., Deuser, W. G., Knauer, G. A. and Lohrenz, S. E.: Rapid coupling of sinking
8 particle fluxes between surface and deep ocean waters, *Nature*, 357(6380), 670–672,
9 doi:10.1038/357670a0, 1992.
- 10
- 11 Auger, P. A., Diaz, F., Ulses, C., Estournel, C., Neveux, J., Joux, F., Pujol-Pay, M. and Naudin, J.
12 J.: Functioning of the planktonic ecosystem on the Gulf of Lions shelf (NW
13 Mediterranean) during spring and its impact on the carbon deposition: a field data and
14 3-D modelling combined approach, *Biogeosciences*, 8(11), 3231–3261, doi:10.5194/bg-
15 8-3231-2011, 2011.
- 16
- 17 Baumann, Z., Fisher, N. S., Gobler, C. J., Buesseler, K. O., George, J. A., Breier, C. F. and
18 Nishikawa, J.: Fukushima 137Cs at the base of planktonic food webs off Japan, *Deep Sea*
19 *Res. Part Oceanogr. Res. Pap.*, 106, 9–16, doi:10.1016/j.dsr.2015.09.006, 2015.
- 20
- 21 Beresford, N., Brown, J., Copplestone, D., Garnier-Laplace, J., Howard, B., Larsson, C.-M.,
22 Oughton, D., Prohl, G. and Zinger, I.: D-ERICA: An integrated approach to the assessment
23 and management of environmental risk from ionising radiation. Description of purpose,
24 methodology and application. A deliverable of the ERICA project FI6R-CT-2004-508847,
25 [online] Available from: <https://wiki.ceh.ac.uk/display/rpemain/ERICA+Tool>, 2007.
- 26
- 27 Brown, J., Dowdall, M., Gwynn, J. P., Børretzen, P., Selnæs, Ø. G., Kovacs, K. M. and
28 Lydersen, C.: Probabilistic biokinetic modelling of radiocaesium uptake in Arctic seal
29 species: verification of modelled data with empirical observations, *J. Environ. Radioact.*,
30 88(3), 289–305, doi:10.1016/j.jenvrad.2006.02.008, 2006.
- 31
- 32 Brown, J. E., Alfonso, B., Avila, R., Beresford, N. A., Copplestone, D., Pröhl, G. and
33 Ulanovsky, A.: The ERICA Tool, *J. Environ. Radioact.*, 99(9), 1371–1383,

1 doi:10.1016/j.jenvrad.2008.01.008, 2008.
2
3 Buesseler, K. O.: Fukushima and Ocean Radioactivity, *Oceanography*, 27(1), 92–105,
4 2014.
5
6 Buesseler, K. O., Jayne, S. R., Fisher, N. S., Rypina, I. I., Baumann, H., Baumann, Z., Breier, C.
7 F., Douglass, E. M., George, J., Macdonald, A. M., Miyamoto, H., Nishikawa, J., Pike, S. M.
8 and Yoshida, S.: Fukushima-derived radionuclides in the ocean and biota off Japan, *Proc.*
9 *Natl. Acad. Sci. U. S. A.*, 109(16), 5984–5988, doi:10.1073/pnas.1120794109, 2012.
10
11 Erichsen, A. C., Konovalenko, L., Møhlenberg, F., Closter, R. M., Bradshaw, C., Aquilonius,
12 K. and Kautsky, U.: Radionuclide transport and uptake in coastal aquatic ecosystems: a
13 comparison of a 3D dynamic model and a compartment model, *Ambio*, 42(4), 464–475,
14 doi:10.1007/s13280-013-0398-2, 2013.
15
16 Estournel, C., de Madron, X. D., Marsaleix, P., Auclair, F., Julliand, C. and Vehil, R.:
17 Observation and modeling of the winter coastal oceanic circulation in the Gulf of Lion
18 under wind conditions influenced by the continental orography (FETCH experiment), *J.*
19 *Geophys. Res.-Oceans*, 108(C3), 8059, doi:10.1029/2001JC000825, 2003.
20
21 Estournel, C., Bosc, E., Bocquet, M., Ulses, C., Marsaleix, P., Winiarek, V., Osvath, I.,
22 Nguyen, C., Duhaut, T., Lyard, F., Michaud, H. and Auclair, F.: Assessment of the amount
23 of cesium-137 released into the Pacific Ocean after the Fukushima accident and analysis
24 of its dispersion in Japanese coastal waters, *J. Geophys. Res.-Oceans*, 117, C11014,
25 doi:10.1029/2012JC007933, 2012.
26
27 Fisher, N. S., Beaugelin-Seiller, K., Hinton, T. G., Baumann, Z., Madigan, D. J. and Garnier-
28 Laplace, J.: Evaluation of radiation doses and associated risk from the Fukushima
29 nuclear accident to marine biota and human consumers of seafood, *Proc. Natl. Acad. Sci.*,
30 110(26), 10670–10675, doi:10.1073/pnas.1221834110, 2013.
31
32 Fowler, S., Buatmenard, P., Yokoyama, Y., Ballestra, S., Holm, E. and Nguyen, H.: Rapid
33 Removal of Chernobyl Fallout from Mediterranean Surface Waters by Biological-Activity,

1 Nature, 329(6134), 56–58, doi:10.1038/329056a0, 1987.
2
3 Fowler, S. W.: Trace elements in zooplankton particulate products, Nature, 269(5623),
4 51–53, doi:10.1038/269051a0, 1977.
5
6 Fowler, S. W. and Fisher, N. S.: Radionuclides in the biosphere, in Marine Radioactivity,
7 vol. 6, pp. 167–203, Hugh D. Livinston, Principality of Monaco. [online] Available from:
8 about:reader?url=http%3A%2F%2Fwww.sciencedirect.com%2Fscience%2Farticle%2F
9 pii%2FS1569486005800075 (Accessed 5 December 2015), 2004.
10
11 Fukuda, S., Iwamoto, K., Atsumi, M., Yokoyama, A., Nakayama, T., Ishida, K., Inouye, I. and
12 Shiraiwa, Y.: Global searches for microalgae and aquatic plants that can eliminate
13 radioactive cesium, iodine and strontium from the radio-polluted aquatic environment:
14 a bioremediation strategy, J. Plant Res., 127(1), 79–89, doi:10.1007/s10265-013-0596-
15 9, 2014.
16
17 Guizien, K., Belharet, M., Marsaleix, P. and Guarinia, J. M.: Using larval dispersal
18 simulations for marine protected area design: Application to the Gulf of Lions
19 (northwest Mediterranean), Limnol. Oceanogr., 57(4), 1099–1112,
20 doi:10.4319/lo.2012.57.4.1099, 2012.
21
22 Harmelin-Vivien, M., Bodiguel, X., Charmasson, S., Loizeau, V., Mellon-Duval, C.,
23 Tronczyński, J. and Cossa, D.: Differential biomagnification of PCB, PBDE, Hg and
24 Radiocesium in the food web of the European hake from the NW Mediterranean, Mar.
25 Pollut. Bull., 64(5), 974–983, doi:10.1016/j.marpolbul.2012.02.014, 2012.
26
27 Hashioka, T. and Yamanaka, Y.: Seasonal and regional variations of phytoplankton
28 groups by top-down and bottom-up controls obtained by a 3D ecosystem model, Ecol.
29 Model., 202(1-2), 68–80, doi:10.1016/j.ecolmodel.2006.05.038, 2007.
30
31 Heldal, H. E., Føyn, L. and Varskog, P.: Bioaccumulation of ¹³⁷Cs in pelagic food webs in
32 the Norwegian and Barents Seas, J. Environ. Radioact., 65(2), 177–185,
33 doi:10.1016/S0265-931X(02)00095-4, 2003.

1
2 Herrmann, M., Estournel, C., Adloff, F. and Diaz, F.: Impact of climate change on the
3 northwestern Mediterranean Sea pelagic planktonic ecosystem and associated carbon
4 cycle, *J. Geophys. Res. Oceans*, 119(9), 5815–5836, doi:10.1002/2014JC010016, 2014.
5
6 IAEA: Sediment distribution coefficients and concentration factors for biota in the
7 marine environment, International Atomic Energy Agency, Vienna, 2004. [online]
8 Available from: [http://www-pub.iaea.org/books/IAEABooks/6855/Sediment-](http://www-pub.iaea.org/books/IAEABooks/6855/Sediment-Distribution-Coefficients-and-Concentration-Factors-for-Biota-in-the-Marine-Environment)
9 [Distribution-Coefficients-and-Concentration-Factors-for-Biota-in-the-Marine-](http://www-pub.iaea.org/books/IAEABooks/6855/Sediment-Distribution-Coefficients-and-Concentration-Factors-for-Biota-in-the-Marine-Environment)
10 [Environment.](http://www-pub.iaea.org/books/IAEABooks/6855/Sediment-Distribution-Coefficients-and-Concentration-Factors-for-Biota-in-the-Marine-Environment)
11
12 Kaeriyama, H., Watabe, T. and Kusakabe, M.: ¹³⁷Cs concentration in zooplankton and its
13 relation to taxonomic composition in the western North Pacific Ocean, *J. Environ.*
14 *Radioact.*, 99(12), 1838–1845, doi:10.1016/j.jenvrad.2008.08.006, 2008.
15
16 Kaeriyama, H., Fujimoto, K., Ambe, D., Shigenobu, Y., Ono, T., Tadokoro, K., Okazaki, Y.,
17 Kakehi, S., Ito, S., Narimatsu, Y., Nakata, K., Morita, T. and Watanabe, T.: Fukushima-
18 derived radionuclides ¹³⁴Cs and ¹³⁷Cs in zooplankton and seawater samples collected
19 off the Joban-Sanriku coast, in Sendai Bay, and in the Oyashio region, *Fish. Sci.*, 81(1),
20 139–153, doi:10.1007/s12562-014-0827-6, 2014.
21
22 Kasamatsu, F. and Ishikawa, Y.: Natural variation of radionuclide Cs-137 concentration
23 in marine organisms with special reference to the effect of food habits and trophic level,
24 *Mar. Ecol. Prog. Ser.*, 160, 109–120, doi:10.3354/meps160109, 1997.
25
26 Kishi, M. J., Kashiwai, M., Ware, D. M., Megrey, B. A., Eslinger, D. L., Werner, F. E., Noguchi-
27 Aita, M., Azumaya, T., Fujii, M., Hashimoto, S., Huang, D., Iizumi, H., Ishida, Y., Kang, S.,
28 Kantakov, G. A., Kim, H., Komatsu, K., Navrotsky, V. V., Smith, S. L., Tadokoro, K., Tsuda,
29 A., Yamamura, O., Yamanaka, Y., Yokouchi, K., Yoshie, N., Zhang, J., Zuenko, Y. I. and
30 Zvalinsky, V. I.: NEMURO—a lower trophic level model for the North Pacific marine
31 ecosystem, *Ecol. Model.*, 202(1–2), 12–25, doi:10.1016/j.ecolmodel.2006.08.021, 2007.
32
33 Kitamura, M., Kumamoto, Y., Kawakami, H., Cruz, E. C. and Fujikura, K.: Horizontal

1 distribution of Fukushima-derived radiocesium in zooplankton in the northwestern
2 Pacific Ocean, *Biogeosciences*, 10(8), 5729–5738, doi:10.5194/bg-10-5729-2013, 2013.
3
4 Komatsu, K., Matsukawa, Y., Nakata, K., Ichikawa, T. and Sasaki, K.: Effects of advective
5 processes on planktonic distributions in the Kuroshio region using a 3-D lower trophic
6 model and a data assimilative OGCM, *Ecol. Model.*, 202(1-2), 105–119,
7 doi:10.1016/j.ecolmodel.2006.08.023, 2007.
8
9 Koulikov, A. O. and Meili, M.: Modelling the dynamics of fish contamination by Chernobyl
10 radiocaesium: an analytical solution based on potassium mass balance, *J. Environ.*
11 *Radioact.*, 66(3), 309–326, doi:10.1016/S0265-931X(02)00134-0, 2003.
12
13 Kryshev, A. I. and Ryabov, I. N.: A dynamic model of Cs-137 accumulation by fish of
14 different age classes, *J. Environ. Radioact.*, 50(3), 221–233, doi:10.1016/S0265-
15 931X(99)00118-6, 2000.
16
17 Kumblad, L., Kautsky, U. and Naeslund, B.: Transport and fate of radionuclides in aquatic
18 environments - the use of ecosystem modelling for exposure assessments of nuclear
19 facilities, *J. Environ. Radioact.*, 87(1), 107–129, doi:10.1016/j.jenvrad.2005.11.001,
20 2006.
21
22 Marsaleix, P., Auclair, F., Floor, J. W., Herrmann, M. J., Estournel, C., Pairaud, I. and Ulses,
23 C.: Energy conservation issues in sigma-coordinate free-surface ocean models, *Ocean*
24 *Model.*, 20(1), 61–89, doi:10.1016/j.ocemod.2007.07.005, 2008.
25
26 Marsaleix, P., Auclair, F. and Estournel, C.: Low-order pressure gradient schemes in
27 sigma coordinate models: The seamount test revisited, *Ocean Model.*, 30(2-3), 169–177,
28 doi:10.1016/j.ocemod.2009.06.011, 2009a.
29
30 Marsaleix, P., Ulses, C., Pairaud, I., Herrmann, M. J., Floor, J. W., Estournel, C. and Auclair,
31 F.: Open boundary conditions for internal gravity wave modelling using polarization
32 relations, *Ocean Model.*, 29(1), 27–42, doi:10.1016/j.ocemod.2009.02.010, 2009b.
33

1 Marsaleix, P., Auclair, F., Duhaut, T., Estournel, C., Nguyen, C. and Ulses, C.: Alternatives
2 to the Robert-Asselin filter, *Ocean Model.*, 41, 53–66,
3 doi:10.1016/j.ocemod.2011.11.002, 2012.
4

5 Mathews, T. and Fisher, N. S.: Trophic transfer of seven trace metals in a four-step
6 marine food chain, *Mar. Ecol. Prog. Ser.*, 367, 23–33, doi:10.3354/meps07536, 2008.
7

8 Petrenko, A., Dufau, C. and Estournel, C.: Barotropic eastward currents in the western
9 Gulf of Lion, north-western Mediterranean Sea, during stratified conditions, *J. Mar. Syst.*,
10 74(1–2), 406–428, doi:10.1016/j.jmarsys.2008.03.004, 2008.
11

12 Povinec, P. P., Hirose, K. and Aoyama, M.: 6 - Pre-Fukushima Radioactivity of
13 the Environment, in *Fukushima Accident*, edited by P. P. P. H. Aoyama, pp. 277–323,
14 Elsevier, Boston. [online] Available from:
15 <http://www.sciencedirect.com/science/article/pii/B9780124081321000061> (Accessed
16 8 May 2015), 2013.
17

18 Rowan, D. J.: Bioaccumulation factors and the steady state assumption for cesium
19 isotopes in aquatic foodwebs near nuclear facilities, *J. Environ. Radioact.*, 121, 2–11,
20 doi:10.1016/j.jenvrad.2012.03.008, 2013.
21

22 Sandberg, J., Kumblad, L. and Kautsky, U.: Can ECOPATH with ECOSIM enhance models
23 of radionuclide flows in food webs? - an example for C-14 in a coastal food web in the
24 Baltic Sea, *J. Environ. Radioact.*, 92(2), 96–111, doi:10.1016/j.jenvrad.2006.09.010,
25 2007.
26

27 Sazykina, T. G.: ECOMOD - An ecological approach to radioecological modelling, *J.*
28 *Environ. Radioact.*, 50(3), 207–220, 2000.
29

30 Sushchenya, L. .: Food rations, metabolism and growth of crustaceans, in *Marine food*
31 *chains*, pp. 127–141, Steele, J.H, Berkeley and Los Angeles., 1970.
32

33 Thomann, R.: Equilibrium-Model of Fate of Microcontaminants in Diverse Aquatic Food-

1 Chains, *Can. J. Fish. Aquat. Sci.*, 38(3), 280–296, 1981.

2

3 Ulses, C., Estournel, C., de Madron, X. D. and Palanques, A.: Suspended sediment
4 transport in the Gulf of Lions (NW Mediterranean): Impact of extreme storms and
5 floods, *Cont. Shelf Res.*, 28(15), 2048–2070, doi:10.1016/j.csr.2008.01.015, 2008.

6

7 UNCEAR: Report to the General Assembly, Scientific Annex a: Levels and Effects of
8 Radiation Exposure due to the Nuclear Accident after the 2011 Great East-Japan
9 Earthquake and Tsunami, in *Sources, Effects and Risk of Ionizing Radiation*, vol. 1, New
10 york., 2014.

11

12 Vives i Batlle, J.: Dynamic modelling of radionuclide uptake by marine biota: application
13 to the Fukushima nuclear power plant accident, *J. Environ. Radioact.*, In press,
14 doi:10.1016/j.jenvrad.2015.02.023, 2015.

15

16 Vives i Batlle, J., Jones, S. R. and Gómez-Ros, J. M.: A method for calculation of dose per
17 unit concentration values for aquatic biota, *J. Radiol. Prot.*, 24(4A), A13,
18 doi:10.1088/0952-4746/24/4A/002, 2004.

19

20 Vives i Batlle, J., Wilson, R. C. and McDonald, P.: Allometric methodology for the
21 calculation of biokinetic parameters for marine biota., *Sci. Total Environ.*, 388(1-3), 256–
22 69, doi:10.1016/j.scitotenv.2007.07.048, 2007.

23

24 Zhao, X. G., Wang, W. X., Yu, K. N. and Lam, P. K. S.: Biomagnification of radiocesium in a
25 marine piscivorous fish, *Mar. Ecol. Prog. Ser.*, 222, 227–237, doi:10.3354/meps222227,
26 2001.

27

28

1 Table 1. Parameter values used in the absorbed dose calculation. All units are in $\mu\text{Gy h}^{-1}$ per
 2 Bq kg^{-1}

Parameter	Definition	Phytoplankton	Zooplankton
$\text{DCC}_{\text{Cs-pk}}$	Dose conversion coefficient for internal exposure	4.7×10^{-6}	4.6×10^{-4}
$\text{DCC}_{\text{Cs-w-pk}}$	Dose conversion coefficient for external exposure	1.1×10^{-4}	3.6×10^{-4}

4
5
6
7

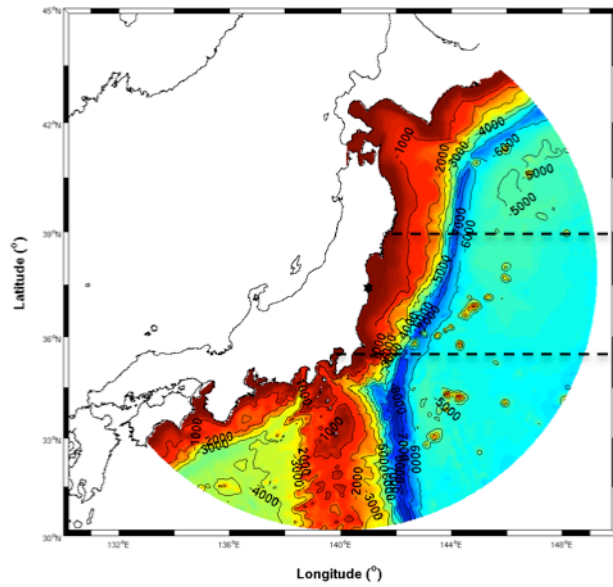
Table 2. Apparent radioecological parameters obtained from the model calibration.

Parameter		Unit	Value
μ_{ps}	Accumulation rate from water for PS	$L g^{-1} d^{-1}$	0.015
μ_{pl}	Accumulation rate from water for PL	$L g^{-1} d^{-1}$	0.015
μ_{zs}	Accumulation rate from water for ZS	$L g^{-1} d^{-1}$	5×10^{-4}
μ_{zl}	Accumulation rate from water for ZL	$L g^{-1} d^{-1}$	5×10^{-4}
μ_{zp}	Accumulation rate from water for ZP	$L g^{-1} d^{-1}$	10^{-3}
λ_{ps}	Small phytoplankton elimination rate	d^{-1}	0.5
λ_{pl}	Large phytoplankton elimination rate	d^{-1}	0.5
λ_{zs}	Small zooplankton elimination rate	d^{-1}	0.11
λ_{zl}	Large zooplankton elimination rate	d^{-1}	0.07
λ_{zp}	Predatory zooplankton elimination rate	d^{-1}	0.03
AE_z	^{137}Cs assimilation efficiency by zooplankton	No dim	0.75

8
9
10
11
12

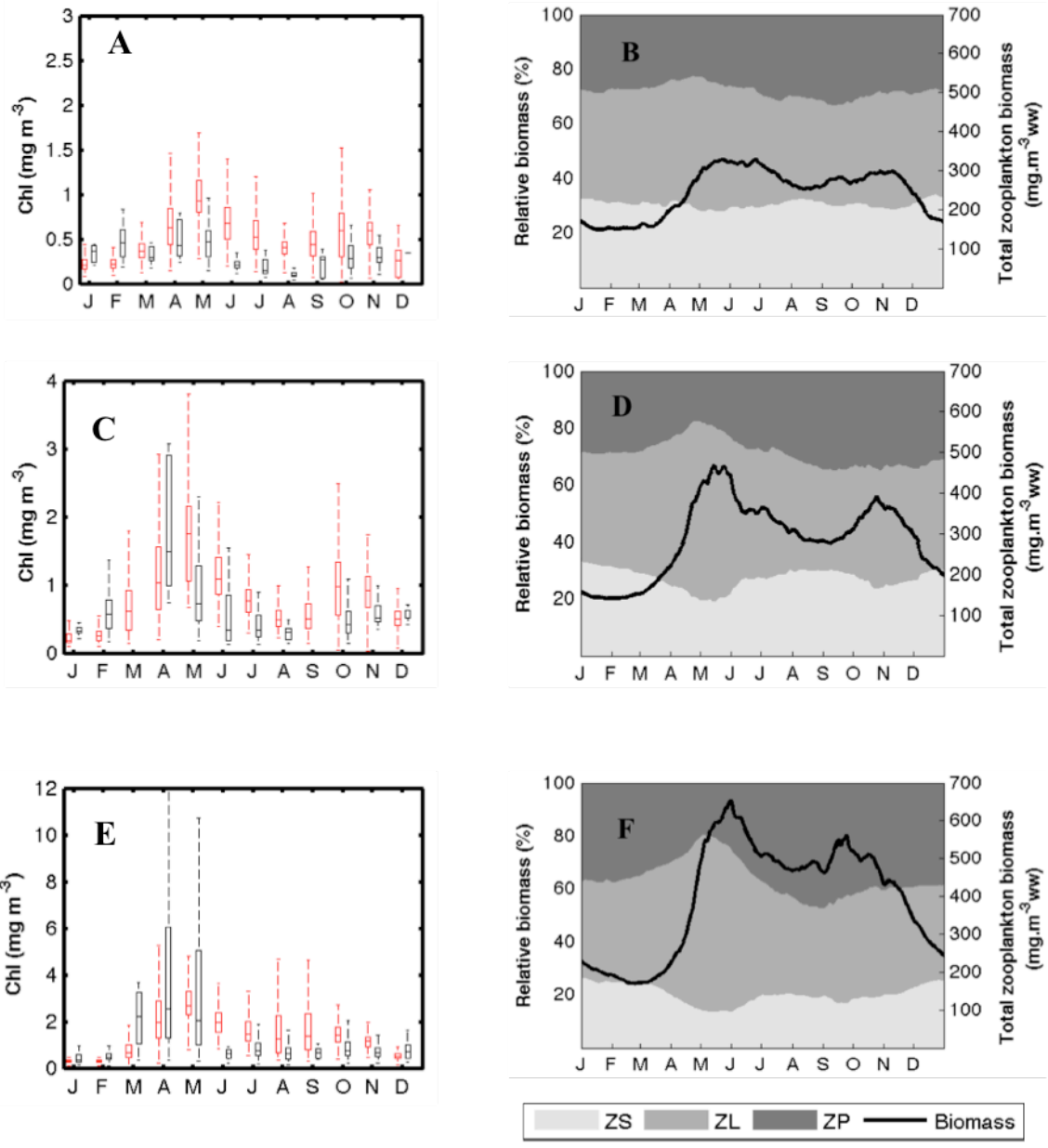
Table 3. Correlation coefficients (r) between the ingestion rates and the TTF of different zooplankton groups.

Parameter	TTF	Non-accidental		Accidental	
		Whole area	0-30 km	Whole area	0-30 km
IR_{ZS}	ZS	0.94	0.91	0.88	0.68
IR_{ZL}	ZL	0.85	0.84	0.77	0.46
IR_{ZP}	ZP	0.83	0.79	0.76	0.37



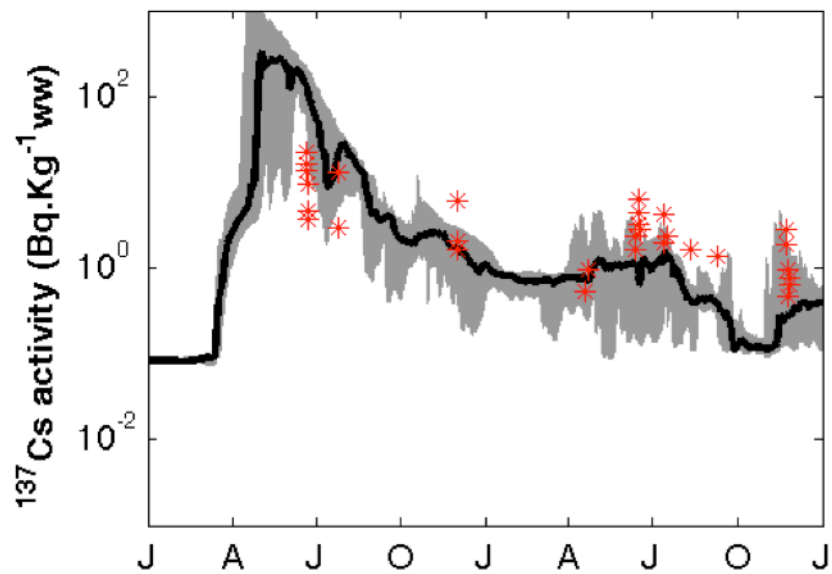
1
2
3
4
5
6

Figure 1. Numerical domain and its bathymetry. The dashed lines indicate the limits of the three regional areas: the subtropical region (latitude < 35°N), the transition region (35°N < Latitude < 39°N), and the subarctic region (Latitude > 39°N).



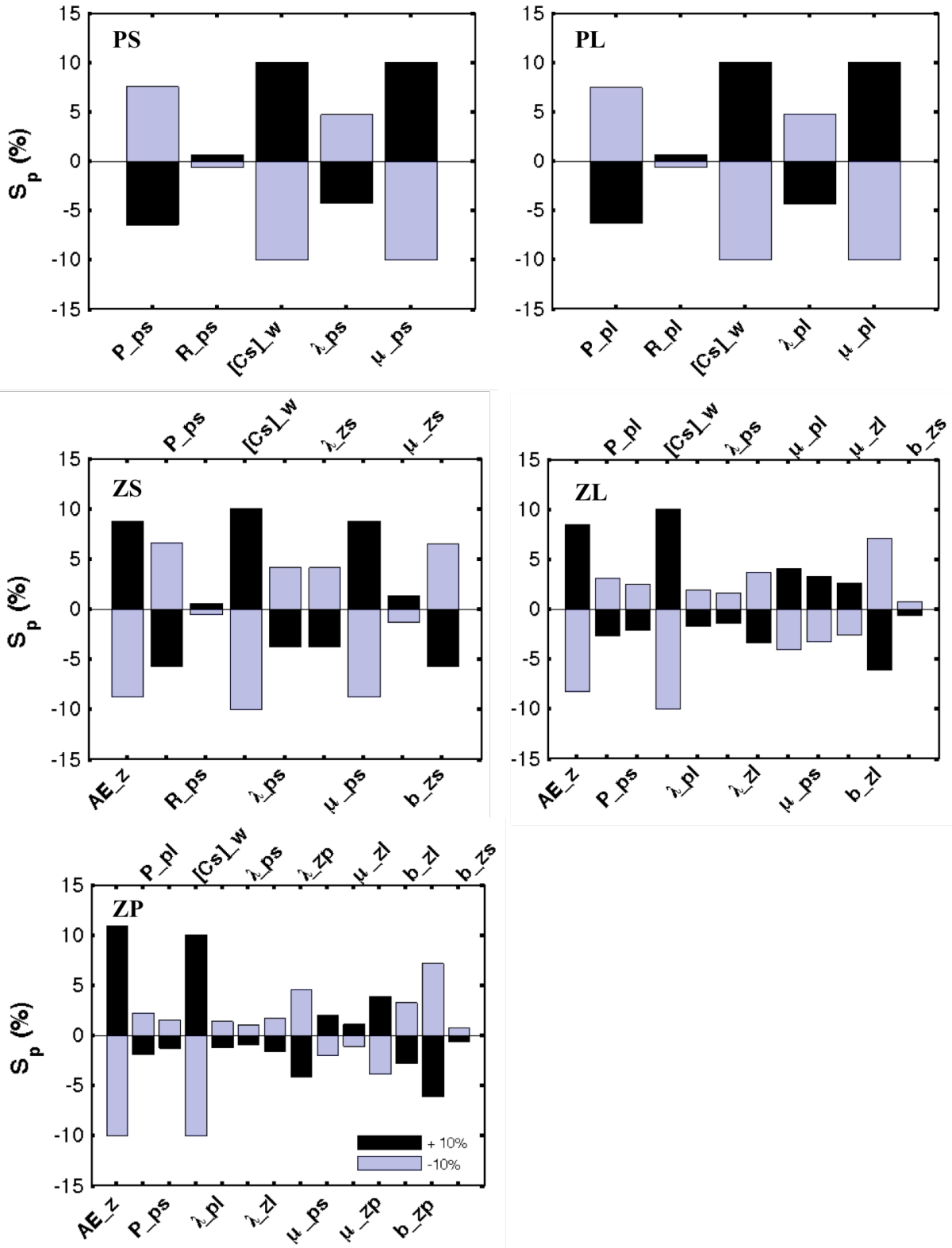
1
2
3
4
5
6
7
8
9
10
11
12

Figure 2. Left (A, C, E): climatological seasonal cycle of integrated chlorophyll from in situ data (in black) and model results (in red) aggregated as monthly medians. In situ climatology data is derived from the Japan Oceanographic Data Center (JODC) dataset for the period (1990-2010). Model outputs are monthly medians for the period 2011-2012 and represented for the three regional areas described in Figure 1. Right (B, D, F): results of the two-year simulation of the total zooplankton biomass represented as the spatial median (dark line) and its taxonomic composition in the three regional areas described above: subtropical region (A, B), transition region (C, D), subarctic region (E, F).



1
2
3
4
5
6
7
8

Figure 3. Results of the model calibration represented as the spatial median of the weighted average of ^{137}Cs concentration in the three zooplankton groups situated in the Sendai Bay. The red stars represent the field data of ^{137}Cs activity in zooplankton in the same location (Kaeriyama et al., 2014).

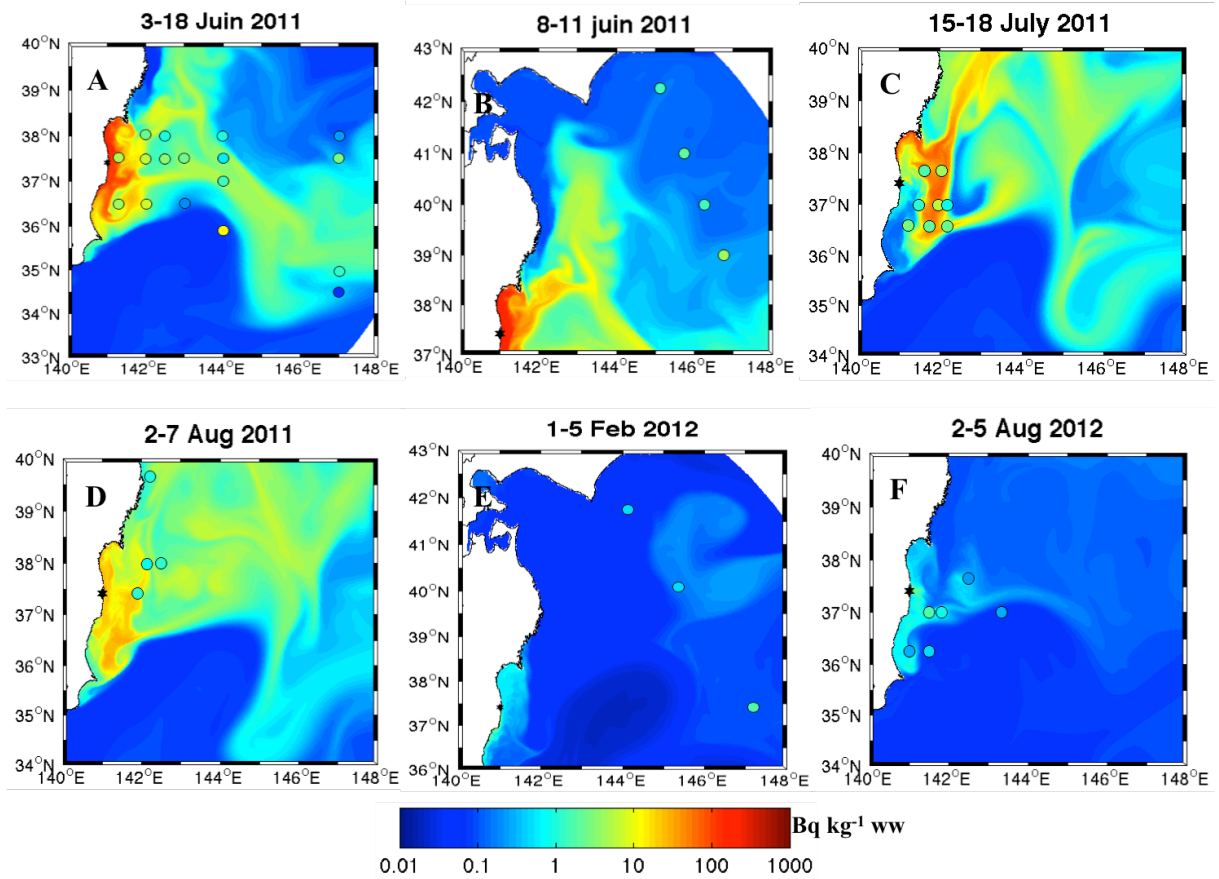


1
2

3 Figure 4. Sensitivity (S_p) of the estimated ^{137}Cs concentrations in different plankton groups
 4 (PS, PL, ZS, ZL, ZP) to a 10% change in the parameters of equations (3) and (7). The S_p
 5 values are calculated using equation (8).

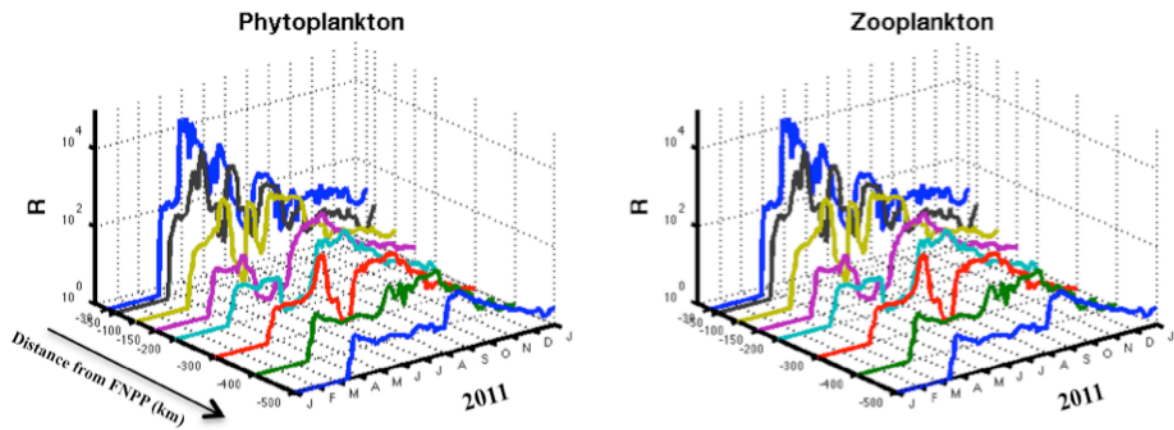
1 Significance of parameters: P_- : primary production rate, R_- : phytoplankton respiration rate,
 2 $[Cs]_w$: ^{137}Cs concentration in seawater, λ_- : depuration rate, μ_- : accumulation rate, AE_z :
 3 Assimilation efficiency, b : growth efficiency of zooplankton.

4
 5



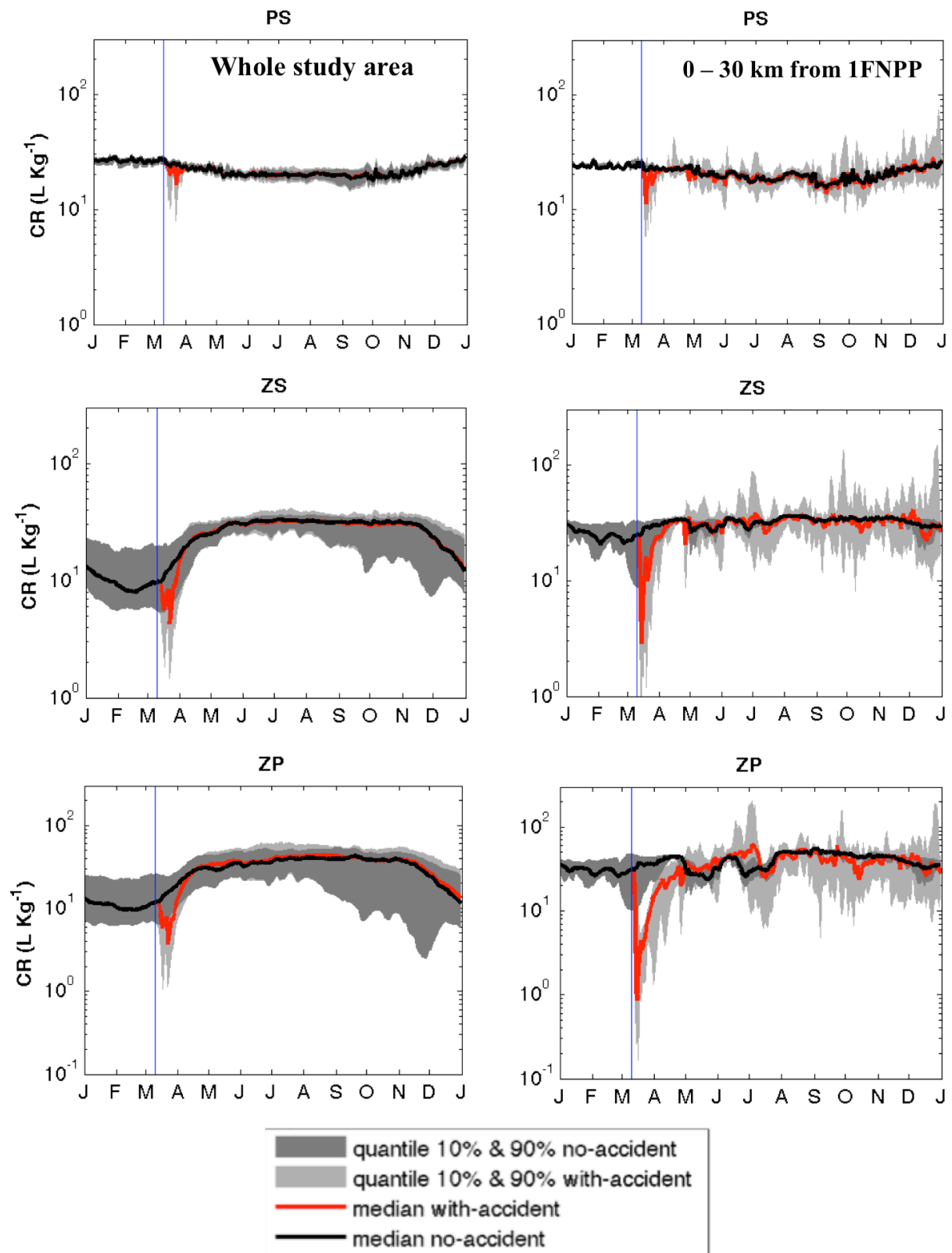
6
 7
 8
 9
 10
 11
 12
 13

Figure 5. Spatial and temporal comparisons between the weighted average of simulated ^{137}Cs concentrations in the three zooplankton groups ($\text{Bq kg}^{-1} \text{ ww}$) and the field observations (colored rounds) reported by (A) Buesseler et al. (2012), (B,C,D,F) Kaeriyama et al. (2014) and (E) Kitamura et al. (2013).



1
2
3
4
5
6

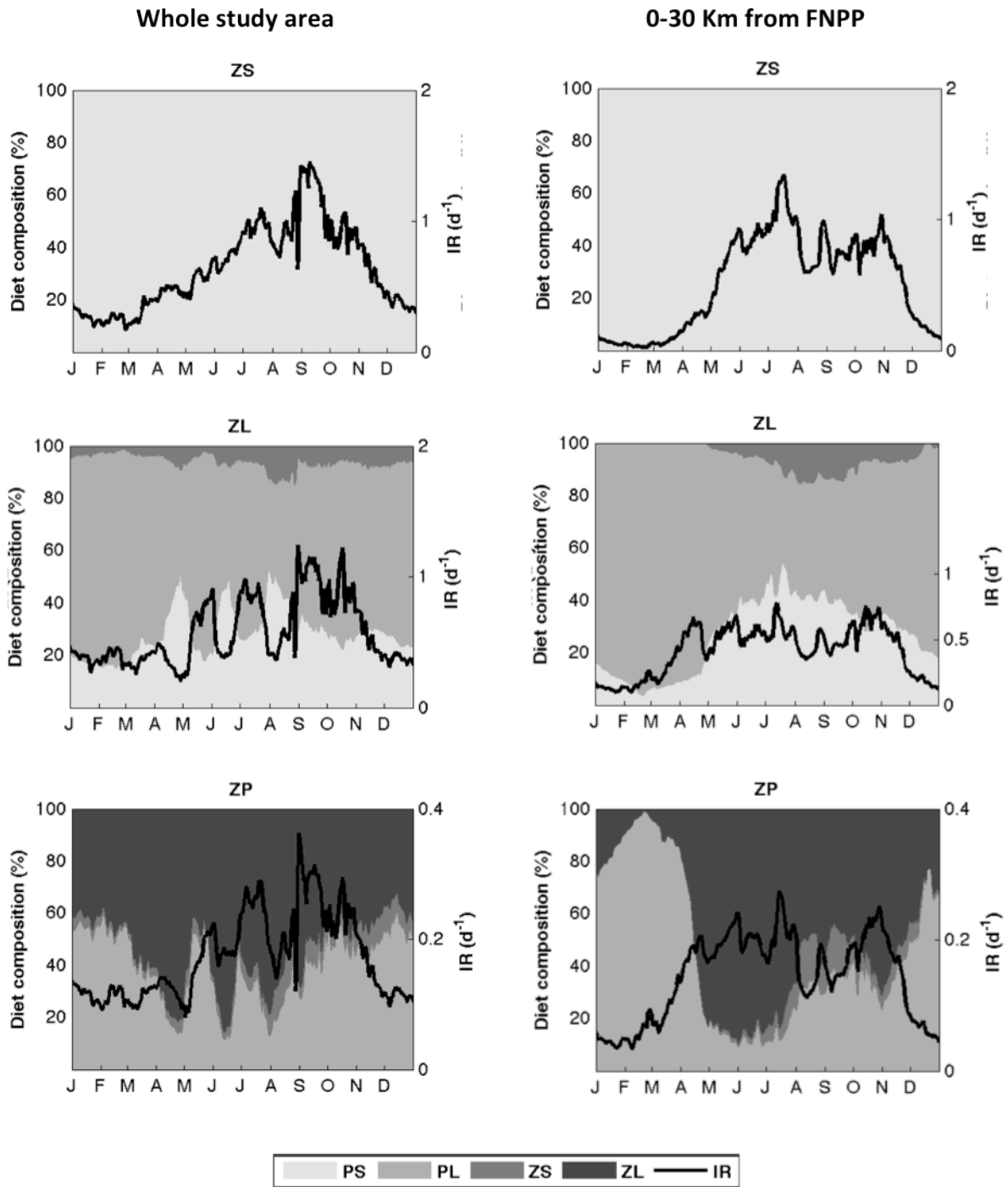
Figure 6. Calculated ratios (R) of ^{137}Cs concentration in phytoplankton and zooplankton in the accident situation to its concentration in the same population in the no-accident situation. The ratio was calculated for different sectors at various distances from FNPP.



1
2
3
4
5
6

Figure 7. Results of concentration ratio estimated for small phytoplankton (PS), small zooplankton (ZS) and predatory zooplankton (ZP) in the whole study area (left) and for those populations located at less than 30 km from FNPP (right). The blue vertical line separates the pre- and post-accident periods.

1



2

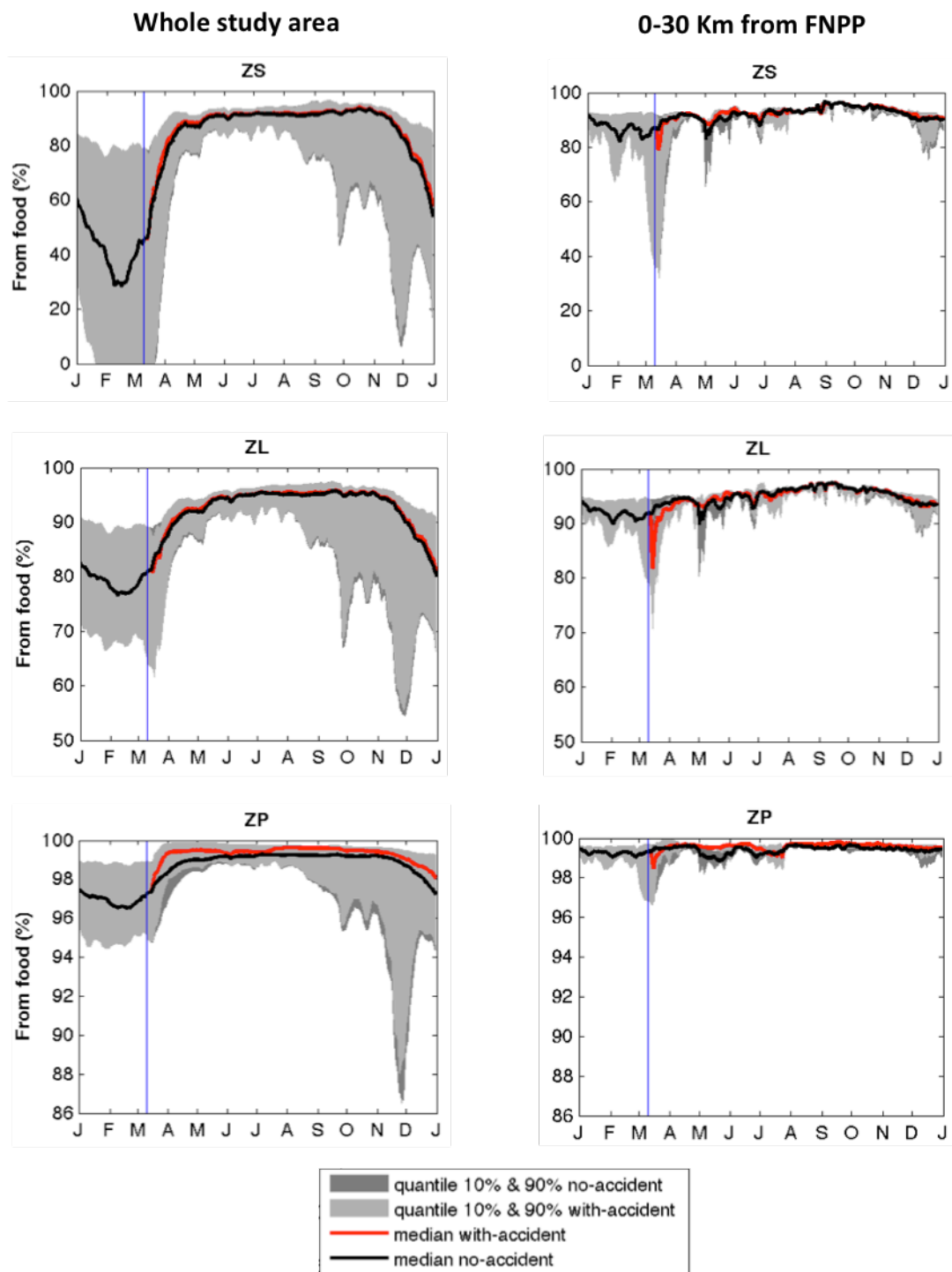
3

4 Figure 8. Food ingestion rate associated with the diet composition for the three groups of
5 zooplankton in the areas located between 0-30 km (left) and for the zooplankton of the whole
6 study area (right).

7

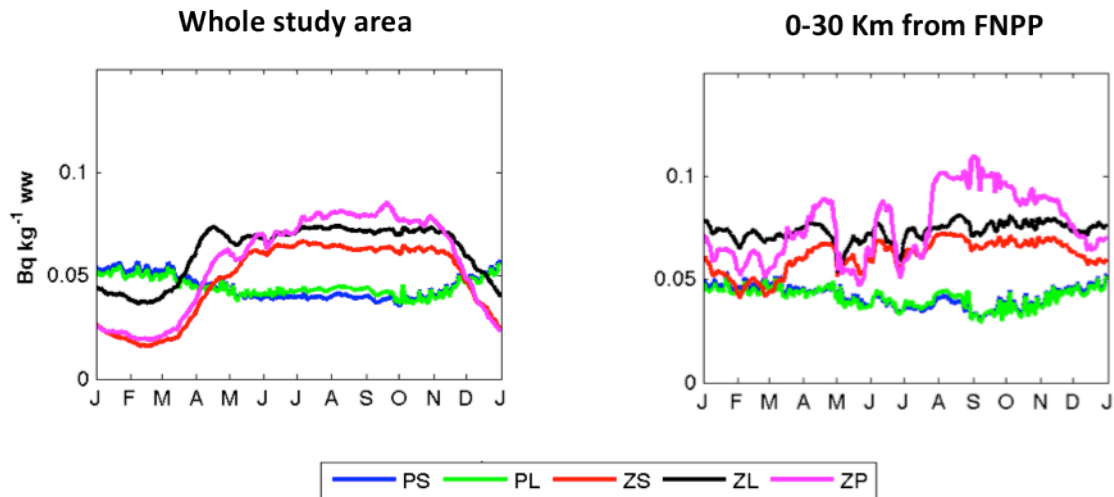
8

9



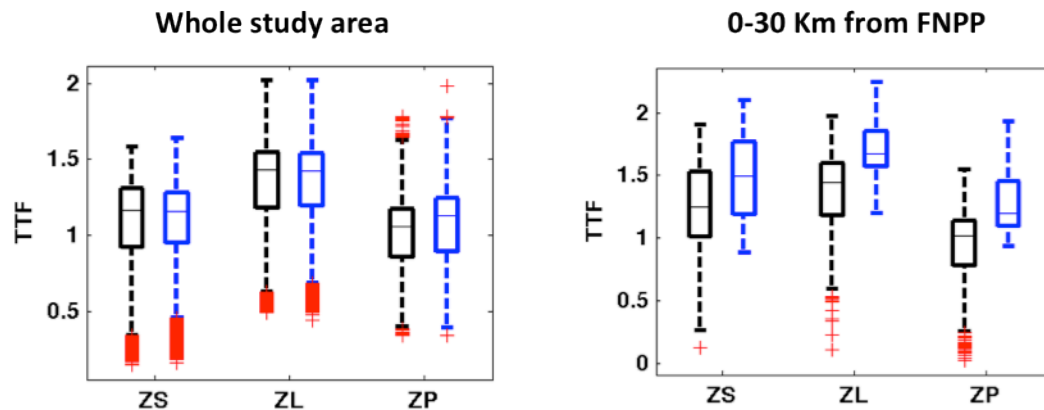
1
2
3
4
5
6
7
8

Figure 9. Relative fraction of ^{137}Cs accumulated from diet for the three groups of zooplankton calculated as the spatial median and quantiles of the whole study area (left) and in the sector located at less than 30 km from FNPP (right). The vertical blue line separates the pre- and post-accident periods.



1
2
3
4
5
6
7

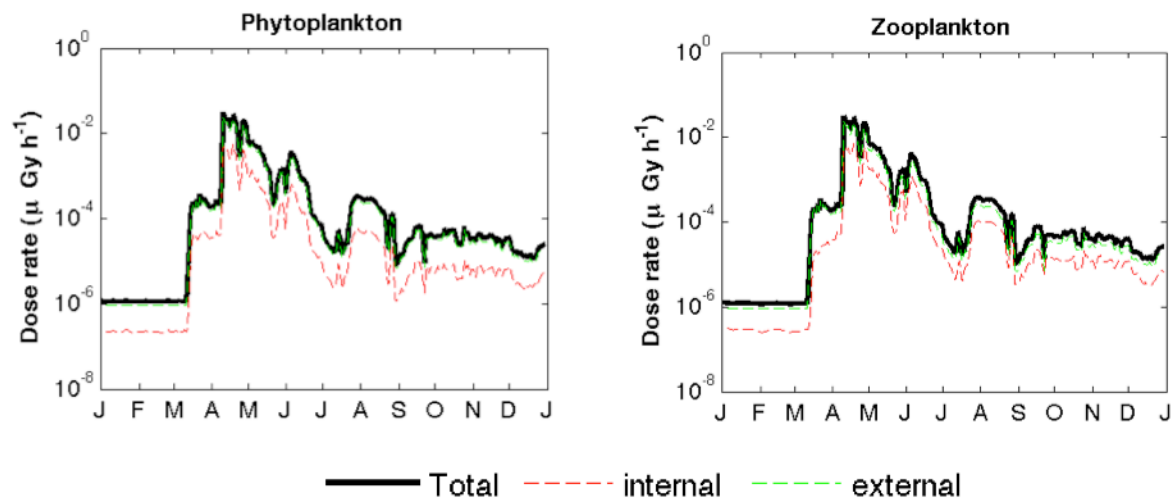
Figure 10: Dynamics of ^{137}Cs concentration in all plankton groups in the no-accident situation.



8
9

10 Figure 11. Boxplots of the Trophic Transfer Factor (TTF) calculated over 2011 for the three
11 groups of zooplankton and for the two different spatial scales. The dark colour represents the
12 accident situation and the blue colour represents the no-accident situation. On each box, the
13 central mark is the median, the edges of the box are the 25th and 75th percentiles, the
14 whiskers extend to the most extreme data points not considered outliers, and outliers
15 are plotted individually (the red marks).

16
17



1
2
3
4
5

Figure 12. ^{137}Cs dose rates received by plankton populations located at less than 30 km from FNPP